Self-assembled gold nanoparticle molecular probes for detecting proteolytic activity *in vivo*

C. Jenny Mu[1,4], **David A. LaVan**[2], **Robert S. Langer**[3], and **Bruce R. Zetter**[4,5,*]

[1] Harvard-MIT Division of Health Sciences and Technology, Cambridge, Massachusetts 02139

[2] National Institute of Standards and Technology, Gaithersburg, MD 20899

[3] Department of Chemical Engineering, Massachusetts Institute of Technology, 45 Carleton Street, Cambridge, Massachusetts 02142

[4] Vascular Biology Program, Children's Hospital Boston, Harvard Medical School, 300 Longwood Avenue, Boston, Massachusetts 02115

[5] Department of Surgery, Harvard Medical School, 300 Longwood Avenue, Boston, Massachusetts 02115

Abstract

Target-activatable fluorogenic probes based on gold nanoparticles (AuNPs) functionalized with self-assembled heterogeneous monolayers of dye-labeled peptides and poly(ethylene glycol) have been developed to visualize proteolytic activity *in vivo*. A one-step synthesis strategy that allows simple generation of surface defined AuNP probe libraries is presented as a means of tailoring and evaluating probe characteristics for maximal fluorescence enhancement after protease activation. Optimal AuNP probes targeted to trypsin and urokinase-type plasminogen activator required the incorporation of a dark quencher to achieve 5 to 8-fold signal amplification. These probes exhibited extended circulation time *in vivo* and high image contrast in a mouse tumor model.

Keywords

Self-Assembly; Gold; Nanoparticles; Near-infrared; Fluorescence; Imaging; Dark Quencher; Proteolysis; Cancer; Tumor

Molecular imaging is an emergent discipline that has the potential to advance integrative biology, promote early detection and characterization of disease, and allow for greater ease in the evaluation of medical interventions. Current implementations of molecular imaging couple the use of existing imaging modalities with unique contrast agents, or molecular probes, designed to target select biomarkers or molecular processes. Specifically, the development of near-infrared fluorescence (NIRF) imaging probes, as essential tools in optical imaging, has enabled researchers to study the real-time dynamics of cellular and biochemical processes *in vivo*. NIRF probe-enhanced optical imaging demonstrates particular promise in cancer diagnosis and treatment and has been applied towards two main areas of interrogation: (1) semiquantitative assessment of biomarker expression levels, and (2) evaluation of pathway-dependent biomolecular activity. Imaging studies to determine pathologic biomarker expression levels typically employ NIRF probes consisting of near-infrared fluorescent molecules or nanoparticles conjugated to affinity ligands, such as antibodies or peptides, to

* Corresponding author bruce.zetter@childrens.harvard.edu.
jennymu@alum.mit.edu, david.lavan@nist.gov, rlanger@mit.edu, bruce.zetter@childrens.harvard.edu

achieve target-specific image contrast and visualization of tumors.[1-7] These same lesions could also be imaged and characterized by their biochemical activity signatures, such as increased proteolysis, using protease-responsive NIRF probes that generate an increased fluorescence signal upon cleavage.[8-10]

One significant advantage of targeting protease activity to convert fluorescently quenched probes to a fluorescent state via proteolysis is the signal amplification capability inherent to the process. Many proteases are known to play essential roles in disease progression, and the ability to directly visualize their physiological activity provides an additional modality for understanding pathogenesis, progression, and treatment effects. However, the process of optimizing NIRF probes, specifically, their quenching efficiency, biocompatibility, targeting ability *in vivo*, and enzyme reaction kinetics, requires a combinatorial approach that proves cumbersome and impractical when applied to existing probe synthesis strategies. Protease-activatable NIRF contrast agents can take the form of single dye-labeled peptide substrates on a synthetic graft copolymer[11-12] or other multivalent support or dual-labeled substrates with dye and quencher/acceptor molecules covalently linked to either terminus.[13-14] The first design represents a homogeneous concentration of fluorescent substrates on a vehicle backbone and relies on self-quenching, while the second configuration implements fluorescence resonance energy transfer (FRET) between dye and quencher/acceptor molecules to suppress the pre-activation fluorescence signal. These strategies require multiple covalent labeling reactions and purification steps and do not allow the ease or modularity of "swappable" components, such as changes in dye molecules.

To address the need for a simple combinatorial method of synthesizing defined NIRF probes, we report the development of fluorescence quenched peptide-based gold nanoparticle (AuNP) probes for the detection of trypsin and urokinase-type plasminogen activator (uPA) proteolytic activities. uPA has been implicated in the progression of multiple cancers, including breast and prostate, by promoting tumor cell invasion, survival, and metastasis. Trypsin was chosen as a simple model protease against which to test the fluorescence quenched AuNPs. Gold nanoparticles (20 nm diameter) were modified with a heterogeneous monolayer of fluorophore and dark quencher-labeled peptide substrates and thiolpoly(ethylene glycol) (SH-PEG; M_W 1000 Da). The fluorophore and dark quencher dyes were chosen to be Quasar 670 (Q670) and BHQ-2, respectively. Peptide substrates were synthesized with a cysteine residue at the C-terminus so that the peptides could passively adsorb onto the gold nanoparticle surface via the sulfhydryl group. Once all labeled substrates and SH-PEG self assemble on the AuNP, effective fluorescence quenching is facilitated by the proximity between fluorophore and dark quencher on the nanoparticle surface as well as the AuNP itself. Figure 1 illustrates the one-step reaction method employed in synthesizing different mixed monolayer surfaces on the AuNP probes and the mode of fluorescence signal generation by target proteolysis of probe surface substrates. Stoichiometric ratios of each surface component at a molar excess over the estimated maximal mole quantity of peptide loading on the 20 nm AuNP surface were varied to generate probe surfaces of differing composition. Dye-labeled peptides and SH-PEG were combined with AuNPs in a single 500 μl reaction mixture and rotated for 16 h at room temperature. Formulation nomenclature is defined as a stoichiometric ratio *X-Y-Z*, where *X*, *Y*, and *Z* are the multipliers for Quasar 670-labeled peptide substrates, BHQ2-labeled peptide substrates, and SH-PEG, respectively, with a common base molar quantity of 3 μM (*e.g.*, 10-2-5 refers to 30 μM Q670-peptide + 6 μM BHQ2-peptide + 15 μM SH-PEG in the reaction mixture). The self-assembled AuNP probes were purified and separated from uncomplexed peptide substrate and SH-PEG by centrifugation and multiple washes with water. AuNP probe activation by the target protease is proposed to effect a de-quenching state by cleavage-specific release of fluorescent and non-fluorescent substrates from the probe surface and subsequent separation of fluorophore and quencher.

Results and Discussion

The self-assembled AuNP probe demonstrated an absorption spectrum bearing strong similarity to that of the bare AuNP, with peak absorbance at approximately 530 nm (Figure 2a). Although no localized surface plasmon resonance (LSPR) band shift was observed for the surface-modified AuNP probe as compared to the bare AuNP, broadening of the absorption spectrum in the longer visible wavelengths reflected the incorporation of BHQ2-labeled and Q670-labeled peptide substrates. The absence of a LSPR band shift indicated that the adsorption of surface components had no appreciable effect on the resulting nanoparticle size, shape, or dielectric constant of the surrounding medium and did not induce AuNP aggregation. Uniform AuNP probe size distribution similar to that of bare AuNPs was observed under transmission electron microscopy (TEM) analysis, demonstrating AuNP probe diameter of ~20 nm (Figure 2b). BHQ2-labeled peptides exhibited a broad extinction profile that extended into the near-infrared wavelengths to overlap with the predicted emission wavelength range of the Quasar 670 fluorophore. Fluorescence emission spectra (λ_{exc} = 400 nm) were collected for unlabeled AuNPs, Q670-labeled and BHQ2-labeled peptide substrates at molar concentrations matched to those of the assembled AuNP probe surface components in water (Figure 2c). As predicted, the BHQ-2 molecule did not fluoresce and acted only as a strong absorber, thus termed a dark quencher. The AuNP probe demonstrated negligible fluorescence and an emission spectrum mirroring that of the unlabeled AuNP. This observation suggests that the combination of BHQ-2 and attachment to the gold surface provides sufficient fluorescence quenching for Quasar 670 emission. Fluorescence suppression is so complete that the only signal detected is attributable to the native emission properties of the unlabeled gold nanoparticle core. Several groups have demonstrated the application of gold nanoparticle-induced fluorescence quenching in biomolecular and cellular detection.[15-19] The primary mode of surface-confined quenching of fluorophores on AuNPs has been identified as a reduction in the radiative rate rather than energy transfer.[20] Studies have shown that strong fluorescence quenching occurs when fluorophores are confined within ~5 nm distance from the nanoparticle surface.[21-22] The surface moieties used in assembling the AuNP probe were expected to fall well within this distance range and benefit from gold-induced quenching. However, since AuNPs are also capable of fluorescence enhancement,[23-24] we hypothesized that the inclusion of a dark quencher on the molecular probe would further reduce the fluorescence background signal, beyond the signal suppression offered by the gold surface.

Several model approaches for evaluating AuNP probe efficacy were considered with the choice of the target protease as the most critical decision. An ideal target protease would be one that has been thoroughly characterized with respect to its biochemical identity, enzymatic activity, and substrate specificity. Specifically, proteases whose substrate preferences have been reduced to synthetic peptide sequences optimized for highly sensitive and specific cleavage reactions provide the greatest advantage in both designing the AuNP probe as well as benchmarking probe performance. Proteases that fulfill these criteria include the family of matrix metalloproteinases (MMPs), caspases, and cathepsins. We chose to assess the contributions of individual surface components to the overall AuNP probe performance by generating a library of trypsin-targeted probes. Trypsin preferentially hydrolyzes peptide bonds at the C-terminal side of arginine and lysine residues. The prevalence of these two amino acids in the proteome enables non-specific trypsin cleavage of many optimized protease substrates. Consequently, initial proof-of-concept and characterization of the AuNP probe library were performed using trypsin as a low-stringency protease target. A prostate-specific antigen (PSA) selective protease substrate, His-Ser-Ser-Lys-Leu-Gln,[25] served as the core peptide sequence for the activatable dye-labeled components on the AuNP probe surface. Q670 (or BHQ2)-(His-Ser-Ser-Lys-Leu-Gln)-Cys substrates were synthesized with the dye conjugated to the N-terminus and a cysteine residue appended to the C-terminus to impart thiol functionalization to the peptide for spontaneous adsorption to AuNPs. Maximum surface peptide density on a

20 nm AuNP was estimated to be 1 peptide/nm^2, resulting in ~1.29 nmol of peptide per pmol of AuNP. The nomenclature used herein to classify different AuNP probe formulations follows the scheme *X-Y-Z*, where *X*, *Y*, and *Z* refer to the molar fold excess over the estimated maximum surface peptide density of Q670-labeled substrate, BHQ2-labeled substrate, and SH-PEG, respectively, in the reaction mixture. Table 1 summarizes the naming convention for the most commonly used probe formulations as the molar fold excess over available AuNP surface attachment sites (the *X, Y,* or *Z* value in the aforementioned nomenclature scheme) and its conversion into the reactant concentration as well as the number of reactant molecules with which each AuNP interacts during the labeling reaction. The values for reactant species concentration in the AuNP labeling process were chosen to span a wide range of molar fold excess over available AuNP surface attachment sites. Typical synthetic peptide modification reactions, for instance, require a 5 to 10-fold excess of the label molecule to drive the process to greater than 90% completion. Consequently, AuNP probe labeling reactions were formulated with a 0 to 5-fold molar excess, or 0 to 15 μM, of each non-fluorescent surface molecule. Since the probe activation signal is directly dependent on the amount of surface bound fluorophore, the upper bound for Q670-substrate concentration in the probe assembly reaction was extended to a 50-fold molar excess, or 150 μM, to preferentially deposit more fluorophore-labeled peptides onto the AuNP surface as compared to the other two surface components. Intermediate reactant concentration values (6, 15, and 30 μM) were then chosen within these ranges to reflect the expectation that the AuNP probe assembly process would progress in a logarithmic fashion with an upper asymptote at which all probe surface sites are occupied.

An activation ratio, or fraction of total possible fluorescence, was determined by measuring the Quasar 670 fluorescence (λ_{exc} = 644 nm; λ_{em} = 670 nm) generated after reacting 1000 U of trypsin with 0.39 pmol of assembled AuNP probe for 30 min and comparing that value to the fluorescence of all surface moieties after being displaced from the nanoparticle surface with dithiothreitol (DTT). The highest activation ratio (36.7 ± 1.4%) was observed for the 50-2-5 AuNP probe, which corresponds to a reaction mixture containing 150 μM Q670-substrate, 6 μM BHQ2-substrate, and 15 μM SH-PEG (Figure 3a). AuNP probes formulated with higher concentrations of Q670-substrate demonstrated a trend towards higher activation ratios, suggesting that the increased availability of Q670-substrate in the formulation mixture leads to greater availability of these same peptides on the nanoparticle surface for trypsin cleavage. Furthermore, the absence of BHQ2-substrates in the reaction mixture results in activation ratios that are much lower than the same AuNP probe formulations with BHQ2-substrates. AuNP probes assembled without BHQ2-substrate exhibited activations ratios that do not extend beyond 15%. To further explore these observations, we examined the activation ratios for the family of AuNP probes formulated with the optimal Q670-substrate concentration (150 μM) more closely for significant trends (Figure 3b). An increase in reaction concentrations of SH-PEG, from 6 μM to 15 μM, improved the activation ratios, independently of the amount of BHQ2-substrates. This observed effect may be attributed to increased hydrophilicity of the AuNP probe surface monolayer and greater probe stability in solution. AuNP probes formulated without SH-PEG precipitated from the aqueous solution, most likely due to the increased hydrophobicity of the probe surface created by the adsorption of multiple dye molecules. In addition, the incorporation of BHQ2-substrates further enhanced the AuNP probe activation ratio, irrespective of the level of SH-PEG reactants. Lee and coworkers have described a similar AuNP probe that utilized Cy5.5-labeled MMP-targeted substrates on the nanoparticle surface and relied on Cy5.5 self-quenching to induce a dark state in the inactivated form.[26] However, the analogous construct in our study, a BHQ2-deficient AuNP probe (50-0-5), demonstrated only 14.9 ± 2.4% recovery of fluorescence after trypsin proteolysis, which represents a greater than 50% reduction from the activation ratio observed for the optimal BHQ2-containing probe (50-2-5).

Under the experimental conditions described herein, self-quenching interactions between adjacent Quasar 670 dyes on the nanoparticle surface did not provide the lowest inactivated fluorescence signal; a dark quencher, such as BHQ-2, was necessary to further suppress the background fluorescence to produce optimal signal and image contrast. Figure 4a illustrates the general trend towards increased signal-to-background ratios in trypsin activation of BHQ2-containing probes over BHQ2-deficient probes, with the best performing nanoparticles exhibiting a greater than 12-fold signal enhancement. To examine the applicability of these observations in the context of a different protease, we constructed a separate library of uPA-targeted AuNP probes in the same manner as the trypsin-targeted probes, using a core substrate sequence of Gly-Gly-Ser-Gly-Arg-Ser-Ala-Asn-Ala-Lys. The activation fluorescence signal after reacting 0.29 pmol AuNP probe with 10 U uPA was compared to the background signal observed for 0.29 pmol AuNP probe without the addition of protease. Similar to the results reported for BHQ-2 influences in the activation of trypsin-targeted probes, uPA-specific probes containing BHQ-2 exhibited a wider dynamic range in activation signal, as illustrated by the expected near unity signal enhancement ratio observed for the 0-2-5 probe as opposed to the 0-0-5 probe, and higher signal-to-background ratios for almost all probe formulations (Figure 4b). However, only a few of the BHQ-2 containing AuNP probes exhibit a statistically significant improvement in the signal-to-background ratios when compared to AuNP probes formulated without BHQ-2 labeled peptides. Large variability in the signal-to-background ratios for both trypsin and uPA targeted AuNP probes may be attributed to the relatively low background fluorescence values exhibited by each probe. As the denominator in this measure of probe performance, small variations in background, or inactivated state, fluorescence result in a much larger and significantly disproportionate change in the signal-to-background ratio. In these functional assays, a relatively dilute probe solution, on the order of 1 nM per reaction, was used, resulting in low detectable background signal. We expect that the use of higher AuNP probe concentrations in the reaction would lead to a significant reduction in signal-to-background ratio variations within the same sample set. In summary, these data suggest that the advantages of incorporating a dark quencher into the AuNP probe, namely additional background signal reduction and enhanced fluorescence recovery, rather than relying exclusively on self-quenching between near-infrared fluorophores, may be generalized to multiple protease targets. A major limitation to this approach may be that the absolute fluorescence signal observed after probe activation may not be as high as in self-quenching probes that do not incorporate a dark quencher, since both quencher and fluorophore molecules are released together from the AuNP probe surface.

Surface composition analysis of trypsin-targeted AuNP probes revealed several characteristics that correlate with probe performance and explain the effects of reaction mixture formulation on surface adsorption. Table 2 outlines the number of surface Q670-substrates and BHQ2-substrates found on purified AuNP probes. After determining the importance of BHQ-2 incorporation and increased SH-PEG reactant levels to probe performance, we investigated the effects of variable Quasar 670 reactant levels on probe surface formation. The addition of more Q670-substrate to the reaction mixture did not result in a monotonic increase in the amount of surface-adsorbed species. At an intermediate concentration of Q670-substrate, between the 20-2-5 and 30-2-5 probes, the ratio of BHQ2-containing substrates to Q670-containing substrates reverses to favor more Quasar 670 molecules on the surface. Furthermore, the total number of dye-labeled peptides on the nanoparticle surface drops between the 20-2-5 and 30-2-5 probe formulations. This phenomenon may be attributed to dimer formation between uncomplexed reactant dye-labeled peptides via their thiol groups at high concentrations in the reaction mixture, precluding their availability for AuNP surface adsorption. AuNP probes that exhibited higher signal-to-background ratios included more dye-labeled substrates on their surfaces, whereas probes demonstrating higher activation ratios, or fluorescence recovery, incorporated fewer dye-labeled substrates. In general, AuNP probes with surface compositions where the BHQ2:Q670 ratios were greater than unity exhibited lower post-activation

fluorescence signals. This observation concurs with the proposed mechanism by which protease-induced probe activation releases both quencher and fluorophore labeled species from the AuNP surface. Once free from surface confinement, the balance between fluorophore and quencher concentrations dictates the resulting fluorescence signal, where a higher level of quencher as compared to fluorophore will result in signal reduction. Signal-to-background ratio optimization requires the AuNP probe to balance a low signal in the inactivated state with high activated fluorescence, which must be supported with an abundance of surface-adsorbed fluorophores. However, this abundance of fluorophores raises two issues for quantifying fluorescence recovery, namely the creation of a large total fluorescence base and increased steric hindrance to the target protease on the nanoparticle surface. In consideration of these seemingly opposing but important measures of AuNP probe performance, we chose the 50-2-5 probe as the optimal formulation based on its sufficiently high signal-to-background ratio and excellent fluorescence recovery. The 50-2-5 probe exhibited the best balance of desired functional characteristics among all of the AuNP probes under consideration. However, alternative probe formulations created by reacting an excess molar ratio of bare AuNPs to surface molecules, rather than the reverse, may be advantageous and promote increased protease cleavage by reducing nanoparticle surface density and thus, steric hindrance to probe activation. Signal-to-background ratios may be further enhanced by synthesizing a non-cleavable peptide or attachment factor for the dark quencher such that only the fluorophore can be proteolytically released from the AuNP probe surface. This probe formulation would benefit from the fluorescence signal suppression offered by the dark quencher at the nanoparticle surface to generate a low background signal. Once the probe was proteolytically activated, only fluorophore molecules would be released into solution without the additional signal reduction effects of simultaneously released quencher molecules.

The determined $k_{cat}\cdot K_m$ for the trypsin-targeted 50-2-5 probe was 1.8 $M^{-1}s^{-1}$ as compared to values on the order of 10^5 $M^{-1}s^{-1}$ reported for uncomplexed peptide substrates.[27] Clearly, the attachment of dye-labeled substrates to a nanoparticle surface at high density greatly impeded proteolytic efficiency, as has been observed by others.[28] Originally designed for imaging PSA activity, these AuNP probes demonstrated such a significant reduction in enzyme reactivity and selectivity as to preclude this application. As determined by Denmeade and coworkers, [25] the $k_{cat}\cdot K_m$ value for the core substrate as an uncomplexed peptide reacted with PSA is 23.6 $M^{-1}s^{-1}$; any further reduction in enzymatic efficiency would render the reaction nearly undetectable within a physiologic context. However, this same inefficiency in proteolysis represents a significant advantage in reducing non-specific degradation of the AuNP probe *in vivo*. Another potential benefit of utilizing AuNPs as vehicle and assembly platform is that their delayed clearance from the circulatory system may allow the protease-specific substrates an extended window of access to target tissues. Circulation time *in vivo* of the 50-2-5 AuNP probe and an equimolar amount of uncomplexed dye-labeled peptide, corresponding to the probe surface composition, was determined by intravenous injection of each species into 6-8 week old athymic nude mice via a lateral tail vein. Serum was collected from each mouse at predetermined time points to measure Quasar 670 fluorescence after DTT treatment of each sample. Rehor and coworkers have suggested that serum levels of intravenously administered nanoparticles within two minutes after injection depict a relatively unperturbed basis for estimating the initial dose.[29] The percentages of initial dose for both probe and uncomplexed peptide retained in serum were calculated by normalizing the fluorescence values at each time point with those determined for serum collected at 1 min post-injection. In the first hour, serum levels of AuNP probe remained high at greater than ~88% of initial dose (Figure 5a). Circulating half-life for the probe was determined to be greater than 4 h. In contrast, more than 90% of the initial administered amount of uncomplexed peptide was removed from serum within the first hour. We modeled explicit circulating levels of each species at $t = 0$ by measuring serum fluorescence after spiking whole blood *ex vivo* with AuNP probe or uncomplexed peptide at the appropriate dilution corresponding to intravenous administration

of 1.16 pmol of probe in a mouse with 2 mL of total blood volume. Over 99% of the uncomplexed peptide was eliminated from serum within the first minute as compared to 64% of intravenously injected AuNP probe (Figure 5b). Using PEG-coated 30 nm diameter gold nanoparticles, Kim and coworkers have also observed significant retention of AuNPs in the circulation with no appreciable loss for at least 4 h.[30] Even greater circulation half-lives have been reported for PEG-coated gold nanorods (~17 h)[31] and ultrasmall superparamagnetic iron oxide nanoparticles (USPIO; 80 min to more than 24 h).[32] In the context of the current literature, these data indicate that peptide substrate attachment to a larger vehicle, such as the AuNP, along with PEG incorporation significantly prolongs its circulation time *in vivo* and support its use via intravenous injection. However, circulation retention time can be further enhanced by changes in nanoparticle shape and modifications in the PEG coating.

The utility of the AuNP probe as an imaging agent *in vivo* was validated using a subcutaneous tumor phantom model in athymic nude mice. The tumor phantom model is an acellular gelated polymer construct that approximates the physical dimensions and anatomic position of a tumor in live animals. Small animal fluorescence imaging of the trypsin-targeted 50-2-5 AuNP probe was performed by mixing 1.16 pmol of functionalized AuNPs or equimolar amounts of the probe components with either Matrigel or PuraMatrix and injecting the solution subcutaneously to form a gelated mass, comparable to the size and shape of a tumor. Since gold nanoparticles demonstrate strong absorption and fluorescence quenching characteristics, probe-equivalent quantities of uncomplexed dye-labeled peptides in the presence and absence of non-functionalized AuNPs were imaged subcutaneously to determine the degree to which AuNPs would suppress fluorescence intensity after simulated release of all surface dye components *in vivo*. Figure 6a is a representative fluorescence overlay image of this experiment, illustrating no significant decrease in signal intensity due to the presence of AuNPs. Trypsin-induced activation of the 50-2-5 AuNP probe was also confirmed in this tumor phantom model by exposing 1.16 pmol of probe to 250 U of trypsin (Figure 6b). The AuNP probe exhibited no significant fluorescence signal in the absence of trypsin with levels that were comparable to those observed for bare AuNPs. These data demonstrate that the AuNP probe is not non-specifically activated by the *in vivo* microenvironment nor does it degrade spontaneously but instead, generates a strong fluorescence signal in the presence of the target protease.

Conclusion

In summary, near-infrared fluorogenic AuNP probes have been characterized and optimized for protease-induced fluorescence enhancement based on functional screens of trypsin and uPA-targeted probe libraries. We described a simple one-step reaction method for producing NIRF AuNP probes with variable surface compositions of dye-labeled peptide substrates and PEG and correlated reactant concentrations with the resulting quantities of adsorbed species on the AuNP probe surface and probe performance *in vitro*. Several design criteria for self-assembled fluorescence quenched AuNP probes emerged from these studies. AuNP probe stability in aqueous solutions was greatly improved by inclusion of 15 μM SH-PEG in the reaction mixture (~6500 molecules of PEG per AuNP). Moreover, incremental increases in the concentration of reactant Quasar 670-labeled peptide substrate beyond 60 mM (~26,000 molecules per AuNP) resulted in a decrease in dye-labeled surface substrates, most likely attributable to dimer formation between uncomplexed reactant substrates. Our most unexpected finding was that the incorporation of a dark quencher, such as BHQ-2, provided additional background signal suppression beyond the fluorescence quenching attributes of the gold nanoparticle and neighboring Quasar 670 fluorophores. Optimized probes designed with the aforementioned criteria were found to exhibit extended circulation time *in vivo*, with $t_{1/2}$ > 4 h, and high image contrast in a subcutaneous tumor phantom model. Although many studies have demonstrated successful development and validation of a multitude of nanoparticle, polymer,[33] and peptide based protease-activatable NIRF probes, few have attempted to

establish design guidelines or generalized principles for constructing optimal imaging agents. To the best of our knowledge, the present study is the first to report on optimization parameters important to probe performance. Future studies will build upon this knowledge and the simple synthesis method introduced in this report to tailor AuNP probes for multiplexed activation and detection as well as therapeutic delivery.

Experimental Methods

Fluorescence Quenched Gold Nanoparticle Probe Synthesis

Gold nanoparticles (Ted Pella, Redding, CA) were pelleted from the stock solution by centrifugation at $10,000 \times g$ for 15 min. The solvent was then replaced with distilled water. HSSKLQC-Wang resin was commercially synthesized (Anaspec, San Jose, CA) and modified with Quasar 670 carboxylic acid and BHQ-2 carboxylic acid (Biosearch Technologies, Novato, CA) at the MIT Biopolymers Laboratory (Cambridge, MA) using standard Fmoc protocol. Dye-labeled uPA substrates with core peptide sequence, GGSGRSANAKC, were also synthesized and modified in the same manner at the MIT Biopolymers Laboratory. Purified Quasar 670 and BHQ-2 labeled peptides were dissolved in distilled water. Stock solution concentrations were determined using absorbance at 579 nm ($\varepsilon = 38,000 \text{ M}^{-1}\text{cm}^{-1}$ for BHQ-2) and 644 nm ($\varepsilon = 187,000 \text{ M}^{-1}\text{cm}^{-1}$ for Quasar 670). Varying stoichiometric ratios of SH-PEG (Nanocs, New York, NY), B-HSSKLQC, and Q-HSSKLQC were added to AuNPs in water to a final volume of 500 µl. The conjugation mixture was rotated end-over-end at room temperature overnight for 16 h. Functionalized AuNPs were pelleted at $10,000 \times g$ for 15 min and washed three times with distilled water. AuNP probes were then stored in water at 4°C.

Transmission Electron Microscopy (TEM)

AuNP probes, formulated as previously described, were deposited onto Cu grids coated with carbon film in a dropwise manner. Images were then obtained using a JEOL JEM-200CX transmission electron microscope operating at 200 kV.

Trypsin Activation Assay

Functionalized AuNPs were pelleted at $10,000 \times g$ for 15 min and solubilized in 600 µl of 2% dimethyl sulfoxide (DMSO) in water (v/v). The solution was then aliquoted (200 µl per well) into opaque 96-well plates (Whatman UNIPLATE). Freshly prepared trypsin (100 U/µl; Sigma-Aldrich, St. Louis, MO) was added at 1,000 U per well concurrent with dithiothreitol (DTT; Sigma-Aldrich, St. Louis, MO) at 10 µl per well and incubated at room temperature for 30 min. Fluorescence measurements for Q670 ($\lambda_{\text{exc/em}} = 644/670$ nm) were made on a Spectramax Gemini M5 spectrofluorometer (Molecular Devices, Sunnyvale, CA).

uPA Activation Assay

Functionalized AuNPs were reconstituted in phosphate-buffered saline (PBS) pH 7.4 to a final nanoparticle concentration of 1.61 nM and aliquoted as 180 µl per well (0.29 pmol AuNP per well) of an opaque 96-well plate (Whatman UNIPLATE). Human urokinase purified from urine (Calbiochem/EMD Biosciences, San Diego, CA) was added to each well in triplicate at 10 U (20 µl of 0.5 U/µl in PBS pH 7.4); 20 µl of DTT was added to separate wells in triplicate for a final concentration of 100 mM per well. Fluorescence kinetic measurements were recorded on a Spectramax Gemini M5 spectrofluorometer immediately after addition of reagents. Endpoint fluorescence measurements for Q670 ($\lambda_{\text{exc/em}} = 644/670$ nm) were made after the microplate reactions had incubated at room temperature for 16 h overnight.

k_{cat}:K_m Determination

AuNP probes (50-2-5) at different concentrations were aliquoted into replicate wells of an opaque 96-well Whatman plate (final concentrations in each well ranging from 773 pM to 11.6 nM). Freshly prepared trypsin was then added at 1000 U per well; fluorescence ($\lambda_{exc/em}$ = 644/670 nm) was then monitored in a spectrofluorometer. Initial release rates of surface substrate were calculated based on a standard curve generated by measuring mixtures of AuNP, BHQ2-labeled and Quasar 670-labeled substrates corresponding to the assayed AuNP probe concentration range. Enzyme kinetics curve fitting was performed using Prism 5.0 software (GraphPad Software, La Jolla, CA) based on the Michaelis-Menten model.

Statistical Analysis

Statistical calculations were performed using Microsoft Excel 2008 for Mac unless otherwise indicated. All graphical data are reported as mean ± standard deviation (s.d.) for the specified number of replicates indicated in the caption. Statistical significance was determined by two-tailed Student's *t* test with 95% confidence for unpaired observations, in the case of circulation retention time comparisons between AuNP probe and uncomplexed peptide, or paired observations for AuNP probe formulation comparisons.

In vivo AuNP Probe Performance

All animal studies were approved by and adhered to guidelines set forth by the Children's Hospital Boston Institutional Animal Care and Use Committee.

Characterization of AuNP Probe Clearance—Total surface dye-labeled substrates on each batch of 50-2-5 AuNP probes were determined by isolating 1 mg of AuNP probe by centrifugation (10,000 × g for 15 min at room temperature). AuNP probe surface components were isolated by addition of 60 μl DTT (1 M stock concentration) followed by 240 μl double-distilled water to the AuNP probe pellet. The reaction was allowed to incubate at room temperature for 16 h. The released surface molecules were collected by centrifuging the reaction at 10,000 × g for 15 min at room temperature. Aliquots (100 μl) of the supernatant were made into a UV-transparent 96-well plate. Absorbance readings were then made as previously described to determine dye composition. Male *Nu/nu* mice (Massachusetts General Hospital, Boston, MA; 6-8 weeks old) were anesthetized using Avertin (240 mg/kg) injected intraperitoneally. 50-2-5 AuNP probe or the equivalent amount of uncomplexed dye-labeled peptide in sterile water was injected intravenously via lateral tail vein (1 mg AuNP probe in 100 μl water per mouse). Mice were euthanized at the specified time points followed by immediate blood collection into BD Microtainer® serum separator tubes (BD Biosciences, Franklin Lakes, NJ). Blood samples were allowed to clot at room temperature for 20-30 min prior to centrifugation at 10,000 rpm for 2 min at room temperature. Aliquots of 100 μl mouse serum were made into each well of an opaque 96-well plate (Whatman UNIPLATE). Dye labeled substrates from AuNP probes in the serum were released from the surface by addition of 40 μl DTT to each well (~286 mM final DTT concentration in each well) and allowed to incubate at room temperature for 16 h. Fluorescence measurements for Q670 ($\lambda_{exc/em}$ = 644/670 nm at 20 reads on medium PMT settings) were made on a Spectramax Gemini M5 spectrofluorometer.

Small Animal Fluorescence Imaging of AuNP Probe Performance with Tumor Phantom Model—Male *Nu/nu* mice (Massachusetts General Hospital, Boston, MA; 6-8 weeks old) were anesthetized under isoflurane. Functionalized AuNPs in sterile water were mixed with PuraMatrix™ (BD Biosciences, Franklin Lakes, NJ) and stored on ice. Immediately prior to injection, 250 U trypsin was mixed with the AuNP/PuraMatrix™ solution. 100 μl of this solution was then injected subcutaneously on each flank. Mice were then imaged using a

Xenogen IVIS 200 system (Caliper Life Sciences, Hopkinton, MA) employing the Cy5.5 filter set ($\lambda_{exc/em}$ = 615-655/695-770 nm).

Acknowledgments

REFERENCES

1. Ballou B, Fisher GW, Hakala TR, Farkas DL. Tumor Detection and Visualization using Cyanine Fluorochrome-Labeled Antibodies. Biotechnol. Progr 1997;13:649–658.

2. Becker A, Hessenius C, Licha K, Ebert B, Sukowski U, Semmler W, Wiedenmann B, Grötzinger C. Receptor-Targeted Optical Imaging of Tumors with Near-Infrared Fluorescent Ligands. Nat. Biotechnol 2001;19:327–331. [PubMed: 11283589]

3. Achilefu S, Dorshow RB, Bugaj JE, Rajagopalan R. Novel Receptor-Targeted Fluorescent Contrast Agents for *In Vivo* Tumor Imaging. Invest. Radiol 2000;35:479–485. [PubMed: 10946975]

4. Moon WK, Lin YH, O'Loughlin T, Tang Y, Kim DE, Weissleder R, Tung CH. Enhanced Tumor Detection using a Folate Receptor-Targeted Near-Infrared Fluorochrome Conjugate. Bioconjugate Chem 2003;14:539–545.

5. Ke S, Wen XX, Gurfinkel M, Charnsangavej C, Wallace S, Sevick-Muraca EM, Li C. Near-Infrared Optical Imaging of Epidermal Growth Factor Receptor in Breast Cancer Xenografts. Cancer Res 2003;63:7870–7875. [PubMed: 14633715]

6. Koyama Y, Barrett T, Hama Y, Ravizzini G, Choyke PL, Kobayashi H. *In Vivo* Molecular Imaging to Diagnose and Subtype Tumors through Receptor-Targeted Optically Labeled Monoclonal Antibodies. Neoplasia 2007;9:1021–1029. [PubMed: 18084609]

7. Lee SB, Hassan M, Fisher R, Chertov O, Chernomordik V, Kramer-Marek G, Gandjbakhche A, Capala J. Affibody Molecules for *In Vivo* Characterization of HER2-Positive Tumors by Near-Infrared Imaging. Clin. Cancer Res 2008;14:3840–3849. [PubMed: 18559604]

8. Tung CH, Bredow S, Mahmood U, Weissleder R. Preparation of a Cathepsin D Sensitive Near-Infrared Fluorescence Probe for Imaging. Bioconjugate Chem 1999;10:892–896.

9. Tung CH, Mahmood U, Bredow S, Weissleder R. *In Vivo* Imaging of Proteolytic Enzyme Activity using a Novel Molecular Reporter. Cancer Res 2000;17:4953–4958. [PubMed: 10987312]

10. Weissleder R, Tung CH, Mahmood U, Bogdanov A Jr. *In Vivo* Imaging of Tumors with Protease-Activated Near-Infrared Fluorescent Probes. Nat. Biotechnol 1999;17:375–378. [PubMed: 10207887]

11. Messerli SM, Prabhakar S, Tang Y, Shah K, Cortes ML, Murthy V, Weissleder R, Breakefield XO, Tung CH. A Novel Method for Imaging Apoptosis using a Caspase-1 Near-Infrared Fluorescent Probe. Neoplasia 2004;6:95–105. [PubMed: 15140398]

12. Jaffer FA, Kim DE, Quinti L, Tung CH, Aikawa E, Pande AN, Kohler RH, Shi GP, Libby P, Weissleder R. Optical Visualization of Cathepsin K Activity in Atherosclerosis with a Novel, Protease-Activatable Fluorescence Sensor. Circulation 2007;115:2292–2298. [PubMed: 17420353]

13. Pham W, Choi Y, Weissleder R, Tung CH. Developing a Peptide-Based Near-Infrared Molecular Probe for Protease Sensing. Bioconjugate Chem 2004;15:1403–1407.

14. Maxwell D, Chang Q, Zhang X, Barnett EM, Piwnica-Worms D. An Improved Cell-Penetrating, Caspase-Activatable, Near-Infrared Fluorescent Peptide for Apoptosis Imaging. Bioconjugate Chem 2009;20:702–709.

15. Shang L, Yin JY, Li J, Jin LH, Dong SJ. Gold Nanoparticle-Based Near-Infrared Fluorescent Detection of Biological Thiols in Human Plasma. Biosens. Bioelectron 2009;25:269–274. [PubMed: 19683912]

16. Prigodich AE, Seferos DS, Massich MD, Giljohann DA, Lane BC, Mirkin CA. Nano-Flares for mRNA Regulation and Detection. ACS Nano 2009;3:2147–2152. [PubMed: 19702321]

17. You CC, Miranda OR, Gider B, Ghosh PS, Kim IB, Erdogan B, Krovi SA, Bunz UHF, Rotello VM. Detection and Identification of Proteins using Nanoparticle-Fluorescent Polymer 'Chemical Nose' Sensors. Nat. Nanotechnol 2007;2:318–323. [PubMed: 18654291]

18. Bajaj A, Miranda OR, Kim IB, Phillips RL, Jerry DJ, Bunz UHF, Rotello VM. Detection and Differentiation of Normal, Cancerous, and Metastatic Cells using Nanoparticle-Polymer Sensor Arrays. P. Natl. Acad. Sci. USA 2009;106:10912–10916.

19. Maxwell DJ, Taylor JR, Nie SM. Self-Assembled Nanoparticle Probes for Recognition and Detection of Biomolecules. J. Am. Chem. Soc 2002;124:9606–9612. [PubMed: 12167056]

20. Dulkeith E, Ringler M, Klar TA, Feldmann J, Javier AM, Parak WJ. Gold Nanoparticles Quench Fluorescence by Phase Induced Radiative Rate Suppression. Nano Lett 2005;5:585–589. [PubMed: 15826091]

21. Dulkeith E, Morteani AC, Niedereichholz T, Klar TA, Feldmann J, Levi SA, van Veggel FCJM, Reinhoudt DN, Moller M, Gittins DI. Fluorescence Quenching of Dye Molecules Near Gold Nanoparticles: Radiative and Nonradiative Effects. Phys. Rev. Lett 2002;89:203002-1-4. [PubMed: 12443474]

22. Aslan K, Perez-Luna VH. Quenched Emission of Fluorescence by Ligand Functionalized Gold Nanoparticles. J. Fluoresc 2004;14:401–405. [PubMed: 15617382]

23. Anger P, Bharadwaj P, Novotny L. Enhancement and Quenching of Single-Molecule Fluorescence. Phys. Rev. Lett 2006;96:113002-1-4. [PubMed: 16605818]

24. Tam F, Goodrich GP, Johnson BR, Halas NJ. Plasmonic Enhancement of Molecular Fluorescence. Nano Lett 2007;7:496–501. [PubMed: 17256995]

25. Denmeade SR, Lou W, Lövgren J, Malm J, Lilja H, Isaacs JT. Specific and Efficient Peptide Substrates for Assaying the Proteolytic Activity of Prostate-Specific Antigen. Cancer Res 1997;57:4924–4930. [PubMed: 9354459]

26. Lee S, Cha E-J, Park K, Lee S-Y, Hong J-K, Sun I-C, Kim SY, Choi K, Kwon IC, Kim K, Ahn C-H. A Near-Infrared-Fluorescence-Quenched Gold-Nanoparticle Imaging Probe for *In Vivo* Drug Screening and Protease Activity Determination. Angew. Chem., Int. Ed 2008;47:2804–2807.

27. Tanaka T, McRae BJ, Cho K, Cook R, Fraki JE, Johnson DA, Powers JC. Mammalian Tissue Trypsin-Like Enzymes-Comparative Reactivities of Human-Skin Tryptase, Human-Lung Tryptase, and Bovine Trypsin with Peptide 4-Nitroanilide and Thioester Substrates. J. Biol. Chem 1983;258:13552–13557. [PubMed: 6358206]

28. Rosi NL, Giljohann DA, Thaxton CS, Lytton-Jean AKR, Han MS, Mirkin CA. Oligonucleotide-Modified Gold Nanoparticles for Intracellular Gene Regulation. Science 2006;312:1027–1030. [PubMed: 16709779]

29. Rehor A, Schmoekel H, Tirelli N, Hubbell JA. Functionalization of Polysulfide Nanoparticles and Their Performance as Circulating Carriers. Biomaterials 2008;29:1958–1966. [PubMed: 18242691]

30. Kim D, Park S, Lee JH, Jeong YY, Jon S. Antibiofouling Polymer-Coated Gold Nanoparticles as a Contrast Agent for *In Vivo* X-Ray Computed Tomography Imaging. J. Am. Chem. Soc 2007;129:7661–7665. [PubMed: 17530850]

31. von Maltzahn G, Park J-H, Agrawal A, Bandaru NK, Das SK, Sailor MJ, Bhatia SN. Computationally Guided Photothermal Tumor Therapy Using Long-Circulating Gold Nanorod Antennas. Cancer Res 2009;69:3892–3900. [PubMed: 19366797]

32. Elias A, Tsourkas A. Imaging Circulating Cells and Lymphoid Tissues with Iron Oxide Nanoparticles. Hematology Am. Soc. Hematol. Educ. Program 2009:720–726. [PubMed: 20008258]

33. Lee S, Ryu JH, Park K, Lee A, Lee SY, Youn IC, Ahn CH, Yoon SM, Myung SJ, Moon DH, Chen X, Choi K, Kwon IC, Kim K. Polymeric Nanoparticle-Based Activatable Near-Infrared Nanosensor for Protease Determination *In Vivo*. Nano Lett 2009;9:4412–4416. [PubMed: 19842672]
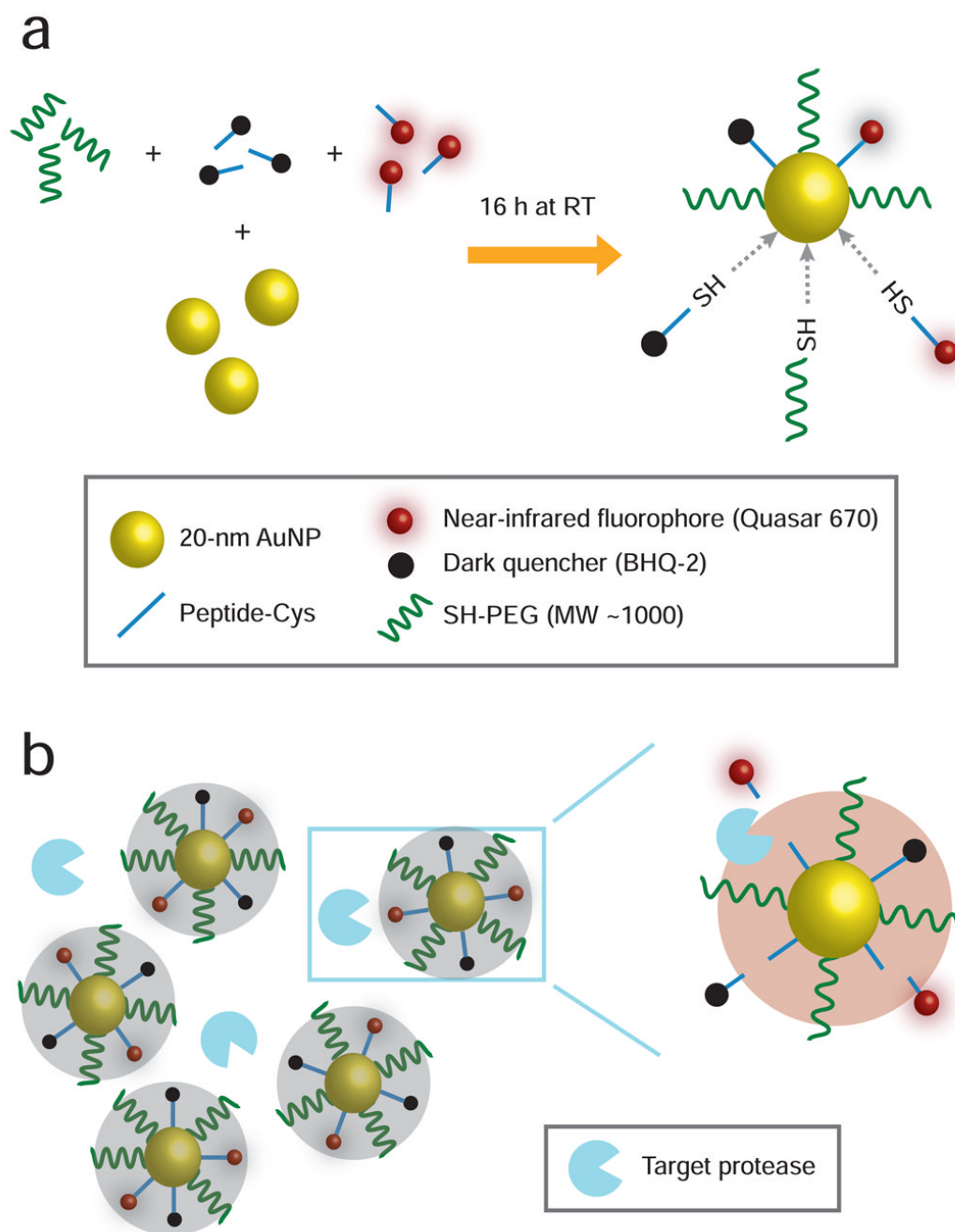
Figure 1.
Schematic diagrams of gold nanoparticle (AuNP) probe synthesis and activation. (a) One-step reaction method for generating self-assembled AuNP probes with different surface compositions, consisting of Quasar 670-labeled and BHQ-2-labeled peptide substrates as well as SH-PEG. (b) Proposed mode of AuNP probe activation by target protease in its conversion from a dark quenched to a near-infrared fluorescent state.
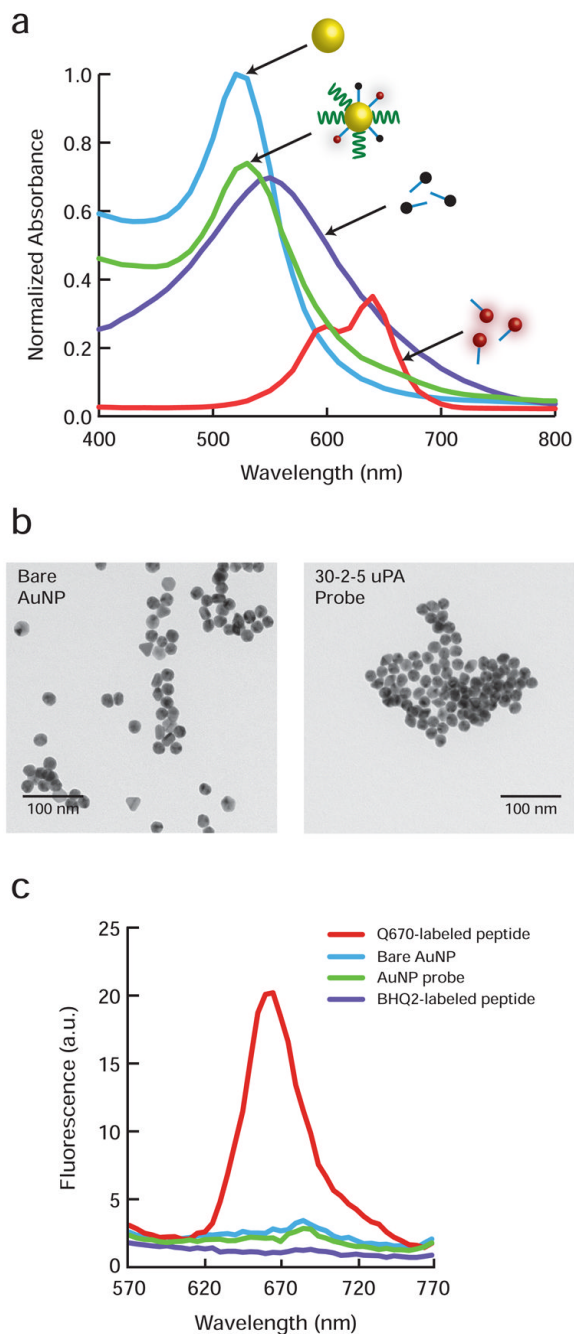
Figure 2.
Photophysical and electron microscopic characterization of gold nanoparticle (AuNP) probes. (a) Absorbance spectra of the self-assembled AuNP probe and its individual components, consisting of a 20 nm diameter AuNP, BHQ2-labeled and Quasar 670-labeled peptide substrates. (b) Representative TEM images of unlabeled 20 nm diameter AuNPs and 30-2-5 uPA targeting AuNP probes. The images were obtained using a JEOL JEM-200CX transmission electron microscope operated at 200 kV. (c) Fluorescence emission spectra (λ_{exc} = 400 nm) of the self-assembled AuNP probe and its individual components.
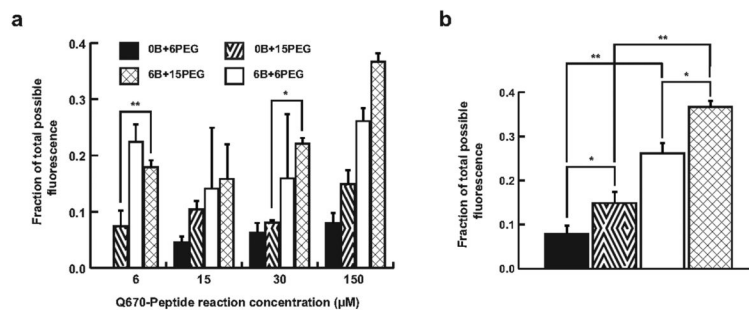
Figure 3.
Trypsin activation assay performed on a library of AuNP probes synthesized with different reaction concentrations of Quasar 670-labeled and BHQ2-labeled peptide substrates and SH-PEG, where "*X*B+*Y*PEG" denotes *X* μM BHQ2-labeled peptide substrates and *Y* μM SH-PEG, to determine the optimal surface composition. Fluorescence activation ratios, defined as the trypsin-activated fluorescence signal with respect to the signal achieved after DTT-mediated release of AuNP probe surface molecules, for (a) a trypsin-specific library of AuNP probes, and (b) the family of AuNP probes generated using reactions containing 150 μM Quasar 670-labeled peptide substrate and varying concentrations of BHQ2-labeled peptide substrates and SH-PEG to determine component-specific contributions to protease-activated signal generation. An increase in the reaction concentration of SH-PEG resulted in an increase in the fluorescence activation ratio (*$p < 0.005$) independent of the BHQ2-labeled peptide substrate reaction concentration. Similarly, the addition of BHQ-2-labeled peptide substrates into the self-assembly reaction (**$p < 0.02$) further enhanced the fluorescence activation ratio independent of SH-PEG reactant concentrations. Trypsin probe formulation, 2-0-2, was not included in this figure, because attempts to purify the AuNP probe after labeling reactions were unsuccessful. All bars represent mean ± s.d. for $n = 3$.
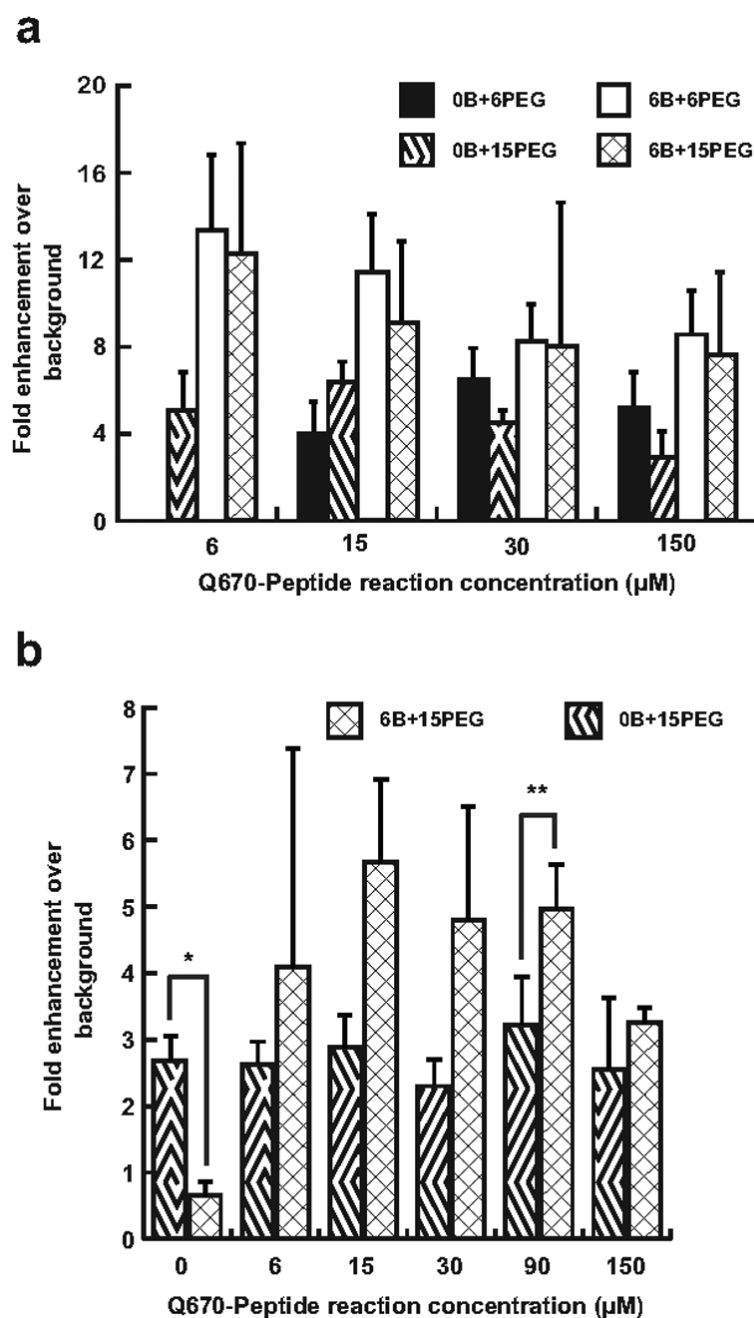
Figure 4.
Protease activation assay performed on a library of AuNP probes synthesized with different reaction concentrations of Quasar 670-labeled and BHQ2-labeled peptide substrates, where "$X\mathbf{B}+Y\mathbf{PEG}$" denotes X μM BHQ2-labeled peptide substrates and Y μM SH-PEG, to determine the optimal surface composition, as measured by the protease-induced fluorescence enhancement over non-activated AuNP probe. (a) Trypsin-activated signal-to-background (S:B) ratios demonstrated a trend towards higher contrast in BHQ2-containing probes. Trypsin probe formulation, 2-0-2, was not included in this figure, because attempts to purify the AuNP probe after labeling reactions were unsuccessful. (b) Urokinase-type plasminogen activator (uPA)-activated S:B ratios. Incorporation of a dark quencher in the AuNP probe synthesis

reaction generated probes with a wider dynamic range, where non-Quasar 670 containing probes exhibited background levels of activation enhancement (*$p < 0.05$). A 5 to 6-fold signal enhancement over background was observed for the optimized probes (**$p < 0.005$). All bars represent mean ± s.d. for $n = 3$.
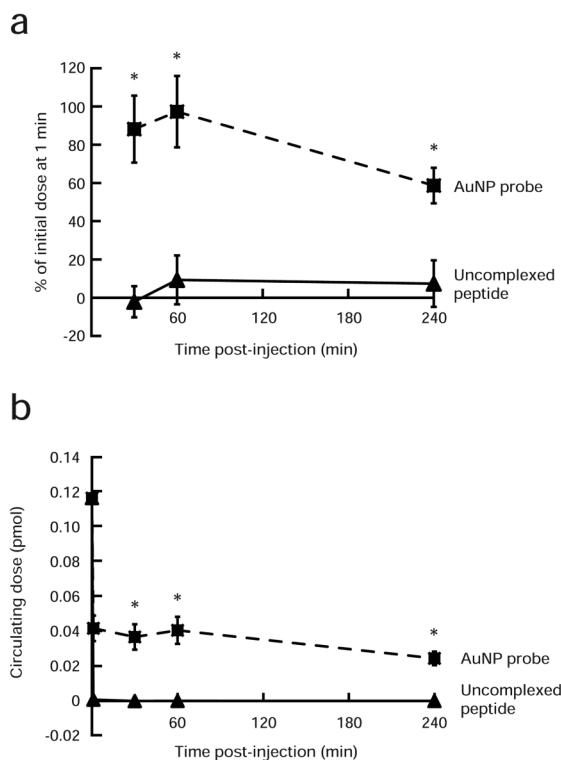
Figure 5.
In vivo circulation retention of AuNP probes as compared to the equivalent mole quantity of uncomplexed Quasar 670-labeled and BHQ2-labeled peptide substrates. (a) Quasar 670 fluorescence detected in serum at each time point was normalized to that measured at 1 min post-injection to arrive at the percentage of the initial administered dose for AuNP probe (■) and uncomplexed peptide (▲). The percentage of AuNP probe retained in the serum remained high during the first hour after injection with circulating half-life, $t_{1/2} > 4$ h. More than 90% of the uncomplexed peptide was removed from serum in the first hour (*$p < 0.001$). (b) The explicit circulating doses of AuNP probe (■) and the equivalent amount of uncomplexed peptide (▲) were determined using Quasar 670 fluorescence. Serum levels of each species at $t = 0$ were estimated by spiking whole blood *ex vivo* with AuNP probe or uncomplexed peptide at the appropriate dilution corresponding to intravenous administration of 1.16 pmol of probe in a mouse with 2 mL of total blood volume. More than 99% of the uncomplexed peptide was eliminated from serum within the first minute after intravenous injection (*$p < 0.001$). Data represent mean ± s.d. for $n = 5$.
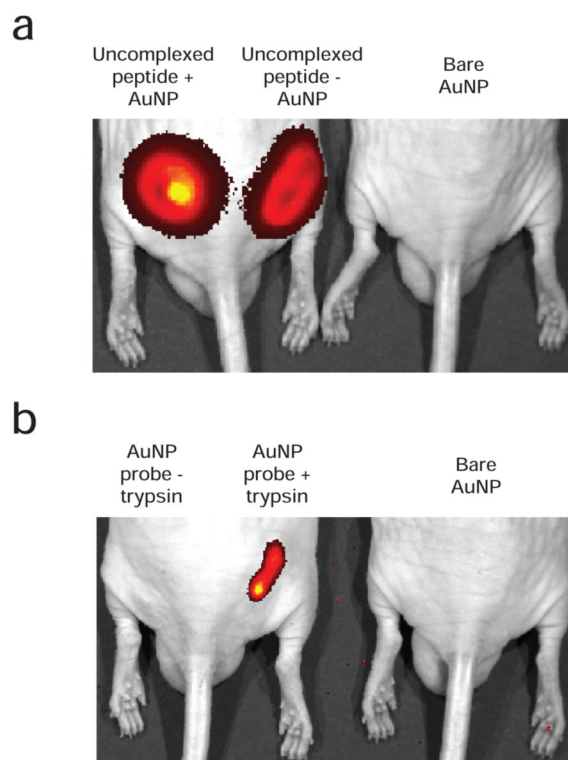
Figure 6.
In vivo near-infrared fluorescence imaging of subcutaneous tumor phantom models consisting of PuraMatrix peptide hydrogel mixed with (a) molar equivalents of uncomplexed Quasar 670-labeled and BHQ2-labeled peptide substrate with and without unlabeled AuNP to simulate the tumor milieu after substrate release from the AuNP probe surface, and (b) 50-2-5 AuNP probe with and without 250 U trypsin as compared to unlabeled AuNPs. Differences in the sizes of fluorescent regions between (a) and (b) reflect only optical artifacts produced by the diffuse nature of fluorescence image acquisition using the Xenogen system when capturing high signal intensity regions. The physical size of the subcutaneous phantom mass in (a) is much smaller than the projected fluorescent signal mapping. Each phantom mass represents the same total injected volume.

Table 1

AuNP Probe Formulation Nomenclature as Converted to Reactant Species (Q670-Substrate, BHQ2-Substrate, or SH-PEG) Concentration and Molar Comparison to Reactant AuNPs

molar fold excess over AuNP surface	reactant species concentration (μM)	no. reactant molecules per AuNP
2	6	~2600
5	15	~6500
10	30	~13 000
50	150	~65 000

Table 2

AuNP Probe Surface Composition as Defined by the Self-Assembly Reaction Concentrations of Quasar 670-labeled Peptide Substrate

formulation [a]	no. Q670-peptide per AuNP	no. BHQ2-peptide per AuNP	BHQ2:Q670 ratio
0-2-5	**	5	**
10-2-5	11	25	2.3
20-2-5	10	26	2.7
30-2-5	4	1	0.33
40-2-5	6	2	0.34
50-2-5	6	2	0.30

[a] Formulation nomenclature is defined as a stoichiometric ratio *X*-*Y*-*Z*, where *X*, *Y*, and *Z* are the multipliers for Quasar 670-labeled peptide substrates, BHQ2-labeled peptide substrates, and SH-PEG, respectively, with a common base molar quantity of 3 μM (*e.g.*, 10-2-5 refers to 30 μM Q670-peptide + 6 μM BHQ2-peptide + 15 μM SH-PEG in the reaction mixture).

** Not applicable.